THE ASTROPHYSICAL JOURNAL, 310:75–85, 1986 November 1

A SPECTROSCOPIC SURVEY OF CASE EMISSION-LINE GALAXIES IN THE DIRECTION OF THE BOOTES VOID

WILLIAM G. TIFFT
Steward Observatory, University of Arizona
ROBERT P. KIRSHNER[1]
Department of Astronomy, University of Michigan
STEPHEN A. GREGORY
Department of Physics and Astronomy, University of New Mexico; and Bowling Green State University
AND
J. WARD MOODY
Department of Astronomy, University of Michigan
Received 1985 November 12; accepted 1986 April 18

ABSTRACT

Redshifts are reported for 44 objects in the list of emission-line objects published by Sanduleak and Pesch in 1982. Two of these are found to be high-redshift quasars, three are galactic stars, three are galaxies with absorption lines only, five are unidentified objects with no emission lines, and the remaining 31 are emission-line galaxies. A wide variety of emission lines strengths is found for each of the Sanduleak and Pesch emission classes except the strongest. The estimated redshifts for galaxies given by Sanduleak and Pesch correlate well with the measured redshifts. The distribution of the emission line galaxies is not homogeneous and is similar to that of galaxies from the CfA survey in the overlapping region. Seven of the galaxies are found near the boundaries of the large Bootes void, and two lie within the void boundaries drawn by Kirshner and colleagues in 1983. The question of whether the void could be populated with low-luminosity galaxies remains unanswered.

Subject headings: galaxies: clustering — galaxies: redshifts

I. INTRODUCTION

The use of medium-sized Schmidt telescopes with objective prisms has been shown to be an important tool (e.g., Smith 1975; MacAlpine, Lewis, and Smith 1977; MacAlpine, Smith and Lewis 1977*a*, *b*; MacAlpine and Lewis 1978) for detecting extragalactic emission-line objects. These objects range in luminosity from high-redshift quasars to small, faint ($M > -14$) galaxies called extragalactic H II regions by Sargent and Searle (1970).

In addition to interest in the intrinsic properties of emission-line objects, their distribution is also of considerable importance. They may provide an easy means for tracing the three dimensional distribution of galaxies. If emission-line galaxies are distributed in the same manner as most of the matter in the universe, their emission lines make redshift observations easy. If they are not distributed in the same manner, they may provide special insight into mechanisms of galaxy formation and environmental influences on galaxy evolution. Sanduleak and Pesch (1982, hereafter SP) interrupted the normal schedule for scanning Burrell Schmidt plates of a large region of the north galactic cap (the Case survey—Sanduleak and Pesch 1983, 1984) in order to publish a survey of 55 emission line-objects in the general direction of the large void in Bootes (Kirshner *et al.* 1981). With rough redshift extimates, SP suggested that six objects in their list might lie in the 12,000–18,000 km s^{-1} redshift range of the Bootes void.

The potential importance of this list caused the Michigan and Steward groups represented in this paper to independently attempt to survey the SP list with spectroscopic observations of sufficient dispersion (typically 250 Å mm^{-1}) to obtain reliable redshifts. This paper represents the result of pooling the data.

II. OBSERVATIONS

The Steward group used the 2.3 m telescope with the pulse-counting Reticon detector. The Michigan group used the McGraw Hill 1.3 m telescope with the Mark II reticon spectrometer, the Kitt Peak 2.1 m telescope with the IIDS detector, and the Kitt Peak 4 m telescope with the HGVS detector. All observations were made in 1982 March or April. Most of the remaining unobserved SP objects (four of seven) are well resolved and thought to have very low redshifts and therefore not important for studies of large scale structure. The reductions proceeded by different programs, but all involved fitting line centers.

Table 1 presents our merged data. The first three columns give the identification number, right ascensiion, and declination, respectively, as listed by SP. The fourth column lists the newly determined redshifts, which contain 300 sin (l) cos (b) corrections for galactic rotation along with Earth's orbital and daily corrections. For galaxies that were observed twice, the quoted redshifts are unweighted means. The redshift of SP 50 has a colon following it which indicates that the poor quality of the spectrum makes line identification very uncertain. The fifth column presents a simple classification of the emission properties determined by the new observations. The emission

[1] Visiting Astronomer, National Optical Astronomy Observatory, which is operated by the Association of Universities for Research in Astronomy, Inc., under contract with the National Science Foundation.

TABLE 1

NEW OBSERVATIONS

SP#	RA (1950)	DEC	V_0 (KM SEC^{-1})	TYPE	TEL.	R1	R2	R3	REMARKS
1	13 58.1	39 9	z=3.3	SE	2.3				QSO
2	14 0.5	39 28	1458	SE	1.3,2.3	0.3	4.3		
3	14 1.2	41 51	10492						ARK
4	14 2.2	40 17	42	ABS	2.3				STAR
5	14 8.6	38 57	7796	SE	1.3,2.3	1.1	2.6	6	
6	14 9.6	39 23	13322	ABS	2.1,2.3				
7	14 13.8	41 13	12534	E	2.3	2.6	3.3	1	ARK
8	14 17.4	40 5	1843	SE	2.3	0.8	3.4	>>1	
9	14 18.2	43 15	19316	ABS/WE	1.3,2.3			2	
10	14 18.2	40 34	7682	WE	1.3				
11	14 19.4	38 22	6780	SE	1.3			6	
12	14 23.1	41 40	25994	WE	1.3				
13	14 24.5	38 37	6877	SE	2.3	0.2	4.9	>>1	
14	14 25.6	38 48							
15	14 27.9	43 9	2618	SE	1.3				
16	14 29.2	40 20	----	--	4.0				NO LINES
17	14 30.3	40 41	6980	SE	2.3	3.2	0.8	5	
18	14 31.8	39 40	-61	ABS	2.3				STAR
19	14 36.2	39 39	-168	ABS	2.3				STAR
20	14 37.9	41 16	5884	SE	4.0				
21	14 38.8	40 52							
22	14 42.3	42 50							
23	14 45.6	38 2	10582	SE	2.1,2.3	1.3	2.5	8	
24	14 48.8	42 57							
25	14 50.4	38 45	4323	SE	2.3	0.9	3.2	4	
26	14 50.6	40 31	8623	SE	4.0				
27	14 53.1	38 20	8428	SE	2.3,4.0	0.2	5.4	>>1	
28	14 56.4	43 3	----	--	4.0				NO LINES
29	14 57.5	42 28	17380	SE	1.3			3	
30	15 4.2	39 24	9400	SE	1.3,2.3	0.3	5.3	>>1	
31	15 4.3	39 22	9174	SE	1.3,2.3	0.3	5.0	>>1	
32	15 4.7	42 50	5396	?					ARK
33	15 5.5	39 16	9204	SE	4.0				
34	15 6.1	43 4	----	--	4.0				NO LINES
35	15 7.7	39 27	4398	E	2.3,4.0	0.8	4.9	>1	
36	15 14.0	42 19							
37	15 16.2	38 24	8900	ABS	2.1				
38	15 16.3	42 55	12043	ABS	2.1				
39	15 16.6	42 23	----	--	4.0				NO LINES
40	15 18.0	39 56	14241	E	2.1,2.3	2.1	1.8		
41	15 18.0	41 1	12492	E	2.1,2.3	3.8	0.7	2	
42	15 19.7	39 22							
43	15 20.5	41 22	z=3.1	SE	2.3				QSO
44	15 22.9	39 34	-----	--	4.0				NO LINES
45	15 24.3	41 50							
46	15 24.7	41 28							
47	15 26.4	40 7	19476	SE	2.1,2.3	0.6	4.3	>>1	
48	15 28.5	41 40	6126	SE	2.1	0.6	3.8	>>1	
49	15 29.7	41 57	8676	SE	2.1,2.3	1.0	3.4	>1	
50	15 34.0	39 4	13747:	VWE	2.3				
51	15 42.6	41 14	9294	?					ARK
52	15 42.8	41 16	9788	SE	2.3	0.9	2.9	8	
53	15 43.8	38 30	8082	SE	2.1,2.3	0.7	3.7	10	
54	15 45.5	40 56	9728	SE	2.3	0.2	4.6	>>1	
55	15 46.0	41 33	10012	SE	2.1,2.3	0.3	11.0	PEC	

NOTES.—(1) R1 is flux ratio of 5007/Hβ; R2 is flux ratio of 3727/5007; R3 is flux ratio of Hα/N II. (2) Also looked at object 12.5 west of SP 6; found no lines. (3) Also looked at object 45″ east of SP 39; found no lines. (4) For SP 27, V_0 = 8460 Steward value; V_0 = 8397 HGVS value. (5) for SP 35, V_0 = 4438 Steward value; V_0 = 4358 HGVS value. (6) Additional identifications: SP 3 = Mrk 283; SP 7 = Mrk 468; SP 8 = Mrk 676; SP 20 = Mrk 1386; SP 24 = Mrk 827; SP 32 = Mrk 480 and NGC 5860; SP 45 = NGC 5929; SP 51 = Mrk 489 and NGC 5992.

strengths range along the progression SE, E, WE, VWE—from strong to very weak emission. SE implies that the counts in the emission peaks are found to be more than twice the peak continuum counts. WE implies that the emission lines are easily identified but are on the order of 10% of the continuum strength. VWE implies uncertainty about whether there is emission or not. A classification of ABS implies that only absorption lines are found. (This type of classification scheme is generally inferior to one based on equivalent widths. In the current sample of observations, however, almost all detectable emission lines in all galaxies were unresolved at the approximately 10 Å resolution of our various spectrograph/detector combinations. Since equivalent widths can be approximated by $[H \times W]/C$ where H, W, and C are line height, width, and continuum measures, respectively [Moody 1986] and since W is unresolved in all cases, our classification system based on H/C is nearly proportional to equivalent width.) The sixth column identifies the telescope sources of the spectroscopic observations. The columns headed R1, R2, and R3 give flux ratios for 5007/Hβ, 3727/5007, and Hα/N II 6584, respectively. Finally, the last column lists remarks about which objects are quasars or stars and those which have earlier redshift determinations by Arakelyan *et al.* (1972, 1973*a*, *b*).

For five SP objects which were observed with the 4 m HGVS system alone, we found no emission or absorption lines. This does not necessarily mean that lines were not present since the wavelength coverage was only 4790 Å $< \lambda <$ 5440 Å, but this region does include the expected wavelengths of Hβ and [O III] lines used as the selection criteria for SP's list. We do not understand why no lines were detected by the HGVS observations of SP 43 but showed N V 1240 in emission at an observed wavelength of about 5200 Å on the 2.3 m spectrum. Perhaps the HGVS observations misidentified the object.

a) Redshift Accuracies

For the Steward Observatory determinations, this paper marks the first publication of results based on a new Reticon reduction program developed by Tifft to support a much larger survey of large-scale structure. A systematic effort is being made to observe a substantial overlap of this larger project with 21 cm redshift lists and with the Center for Astrophysics survey (Huchra *et al.* 1983, hereafter CfA) in order to determine accuracies; this effort will be reported later. Preliminary results are as follows: We have measured redshifts for NGC 5548, NGC 4670, NGC 6166a, and NGC 4881 (three determinations). The first two galaxies mentioned are strong emission-line objects. We differ from 21 cm observations (quoted by Huchtmeier *et al.* 1983) by -77 km s^{-1} and $+47$ km s^{-1}, respectively. NGC 6166a and NGC 4881 are primarily absorption-line objects; we differ from earlier photographically recorded data by $+157$ km s^{-1} (Minkowski 1961) and $+55$ km s^{-1} (Tifft and Gregory 1976) respectively. As preliminary statements, we believe that these new determinations show no systematic error, that emission-line redshifts are probably accurate to about 65 km s^{-1}, and that absorption line redshifts are probably accurate to better than 100 km s^{-1}.

The Michigan data were first reduced using a single-dispersion fit along the whole spectrum. Systematic errors led to a reanalysis using separate blue and red fits (as is done at Steward) for the data from the 1.3 and 2.1 m telescopes. For 11 E or SE overlapping redshift determinations, we find the mean value of Steward minus new Michigan values to be $\langle SO - M \rangle = 29 \pm 64$ km s^{-1}. Therefore, there is no substantial difference between the final Michigan and Steward values. We do not have the same degree of confidence in the 4 m HGVS data.

III. RESULTS

a) SP Emission Classifications

SP included an emission strength classification which is generally similar to ours; their system ranged from S (strong) to W? (weak and uncertain). Table 2 compares their classification results with ours. For at least three reasons, one does not expect a one-to-one mapping of classification systems. First, our dispersions are at least 7 times greater than that used by SP. Second, we often observed O II as well as O III, whereas SP concentrated on O III. Third, it is very difficult for low-dispersion objective prism techniques to determine the continuum strength. The SP classifications are found to be reliable only for the strongest emission class. For all other bins of the SP scheme, we find spectra as diverse as SE and ABS, but the general trend is for more agreement on the strongest lined objects. Therefore, any galaxy in which SP can reliably detect an emission line is likely to belong to our SE (strong emission) class.

b) High-Redshift Quasars

By searching for suspected [O III] emission within the wavelength range 5000–5350 Å, the Case survey method also will pick up high-redshift quasars; for Lyα this gives a range of $3.1 < z < 3.4$. Although SP claim to have tried to exclude an unknown number of quasar candidates from their list, two of the objects have been verified as quasars.

SP 1 shows broad Lyα emission at $\lambda \approx 5200$ Å yielding $z \approx 3.3$. There is evidence for narrow absorption on the blue side of the emission peak. The only other clear line in this spectrum is a blend of Lyβ and O VI at an observed wavelength of $\sim$4400 Å.

SP 43 is a broad absorption line (BAL) quasar. Its spectrum shows a broad emission feature at an observed wavelength of $\sim$5200 Å and a very broad absorption trough blueward of the emission. We interpret these features to represent N V 1240 Å emission with the Lyα feature completely masked by the broad absorption. This is a common characteristic of BAL quasars and yields a redshift of $z \approx 3.1$.

c) SP Redshift Estimates

Using the distance between 3727 Å and 5007 Å, SP provided rough estimates (to the nearest 0.01 in z) of redshifts for galaxies that showed emission from both [O II] and [O III]. It was these estimates along with four previous redshifts from Arakelyan *et al.* (1972, 1973*a*, *b*) that allowed SP to suggest that six

TABLE 2

EMISSION CLASSIFICATIONS[a]

	SP			
NEW	W?	W	M	S
SE	5	7	10	3
E	1	1	2	0
WE	0	1	1	0
VWE	0	0	1	0
ABS	3	2	2	0

[a] See text for explanation of classification systems.

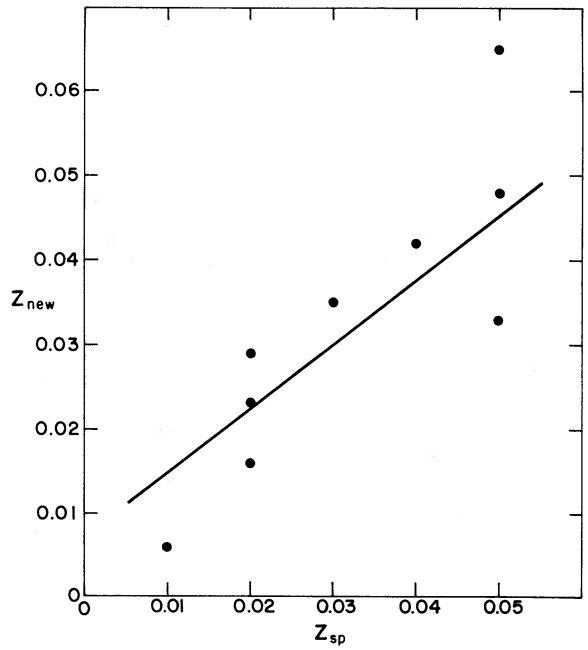

FIG. 1.—A plot of newly determined accurate redshifts (vertically) vs. SP estimated redshifts. The SP estimations are reasonably accurate but tend to overestimate the redshift.

of their galaxies might lie in the redshift range of the Bootes void.

There are nine galaxies that have both newly determined accurate redshifts and SP redshift estimates. In order to test the accuracy of the SP estimates, we performed a linear least-squares solution of z_{new} on z_{SP}. The results are $z_{new} = 0.76 z_{SP} + 0.01$, with a correlation coefficient of $r = 0.86$. Figure 1 shows a plot of z_{new} versus z_{SP}.

d) Large-Scale Structure

Figure 2 shows a stereographic projection of the SP sample on the sky. We will sort out the three-dimensional structure of this data set in three ways—wedge diagrams, selected redshift slices, and supplemental data samples.

Figure 3 is a wedge diagram of the data extending out to a redshift of 25,000 km s^{-1}. CfA data ($m_p < 14.5$) in the SP survey area have been added as open circles in order to add detail to the nearer regions. We note that seven SP galaxies have redshifts in the range (12,000 $< V_0 <$ 18,000 km s^{-1}) of the Bootes void. Only two galaxies are found in the redshift range $V_0 >$ 18,000 km s^{-1} (beyond the void). In addition to the normal Malmquist bias inherent in any magnitude limited sample (for the Case survey this limit is unknown), an additional effect enters into the SP data. For the Case technique, the presence of [O III] was used as a criterion for inclusion, but at $z > 0.06$ 5007 is shifted to beyond 5300 Å where the sensitivity of the IIIa-J emulsion drops sharply.

Figure 4 is an expanded view of figure 3 and only extends to a redshift in 15,000 km s^{-1}. This has been included in order to help map out the nearer structure.

Figure 5 shows a map of the distribution of CfA galaxies in an expanded region containing the SP sample area. The plotted numbers represent the galaxies' redshifts truncated to units of 10^3 km s^{-1} and are centered upon the galaxies' positions on the sky. Since Figure 5 is visually confusing, we present Figures 6–8, which are 3 "slices" in redshift. Figures 6 and 7 strongly suggest the presence of at least two filaments. One of these runs primarily north-south at $\alpha = 14^h.5$; the other one runs primarily east-west at $\delta = 43°$. These filaments appear in this diagram to be at least 15 h^{-1} Mpc^{-1} (where $h = H_0/100$ km s^{-1} Mpc^{-1}) in extent. (These estimates are lower limits since they represent the boundaries of the diagram only.) Figure 8 also suggests a higher redshift filament running from $\alpha = 16^h.3$, $\delta = 35°$ to $\alpha = 15^h.5$, $\delta = 45°$. We will refer to these filaments by their redshifts. Hence they will be termed the 3K, 5K, and 9K filaments, respectively. Assuming pure Hubble flow, the characteristic depths of the filaments are about 4 h^{-1} Mpc^{-1}. For comparison, this length scale corresponds to about 5° at the distance of the 5K filament in Figure 7. The length of the 5K filament appears to be at least 25°, and its apparent width as projected on the sky is $< 5°$.

We reiterate that the CfA data sample was introduced in order to help delineate structures found in the narrowly shaped SP sample region and to compare these two differently chosen samples. Figures 2 and 4 can be interpreted directly by comparison with Figures 6–8. The east-west 5K filament nearly coincides with the narrow SP sample region and is well represented in Figure 4. The 9K filament in Figure 8 either ends at $\alpha = 15.5$ or, unlikely, includes the more westerly objects in Figure 8, but these latter objects lie generally south of the SP region. The galaxies with $2000 < V_0 < 4999$ km s^{-1} form a complicated filamentary structure which is not delineated satisfactorily by either the maps or wedge diagrams.

A small diameter (25 h^{-1} Mpc^{-1}) void is suggested by both Figures 4 and 5 centered at $\alpha = 15^h.2$, $v \approx 7000$ km s^{-1}.

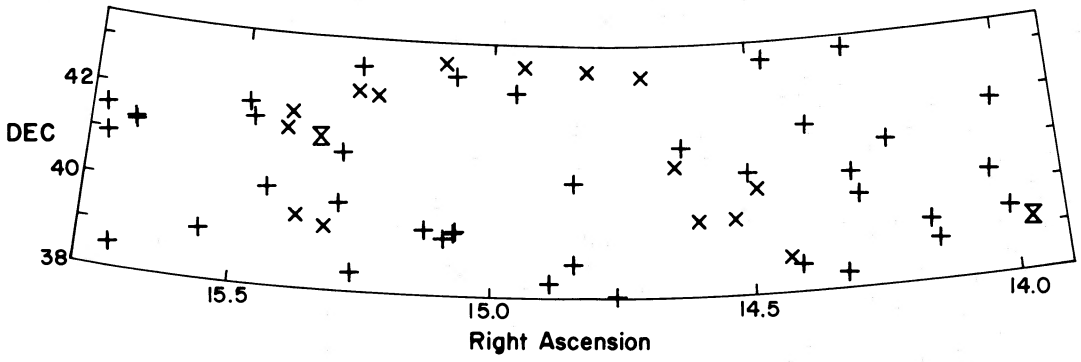

FIG. 2.—A stereographic projection of the positions of the SP galaxies on the sky. Large X's represent two high-redshift quasars. Plus signs represent SP objects with known redshifts. Small X's represent unobserved SP objects; these are mostly very nearby galaxies with large diameters.

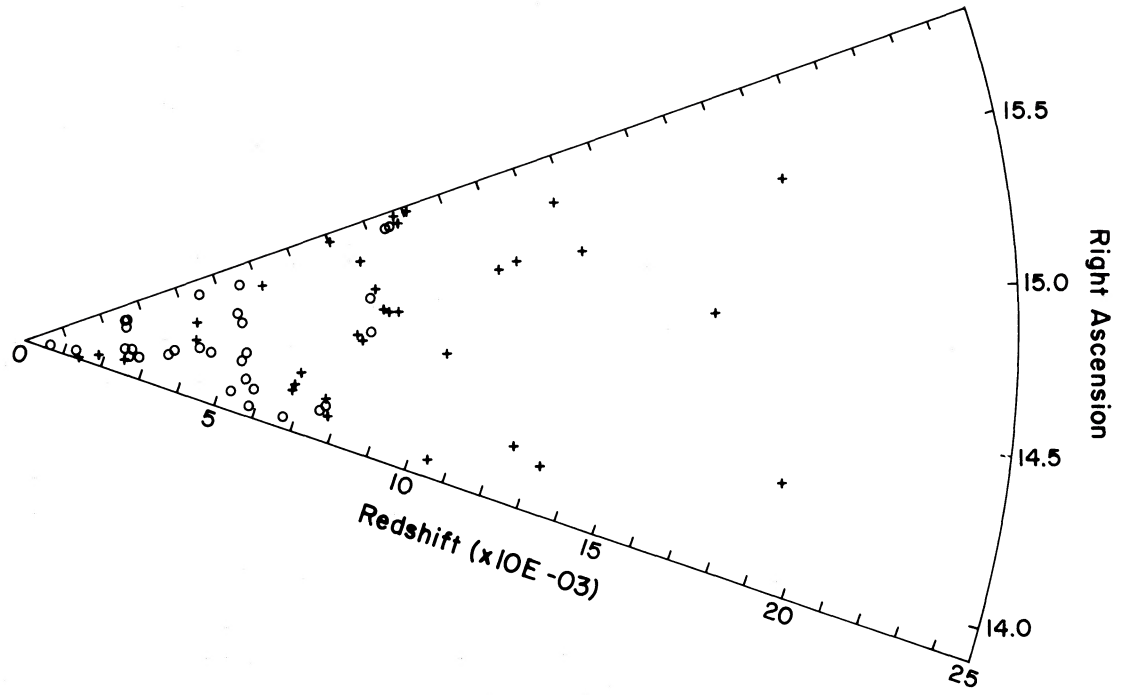

FIG. 3.—A wedge diagram of the SP data (*plus signs*) along with CfA galaxies (*open circles*) in the same region of the sky. One can see that the CfA objects do not provide much large-scale structure data beyond 5000–10,000 km s^{-1} redshifts. The Bootes void at 12,000–18,000 km s^{-1} is not substantially filled by these data, but it is not overwhelming in this sample.

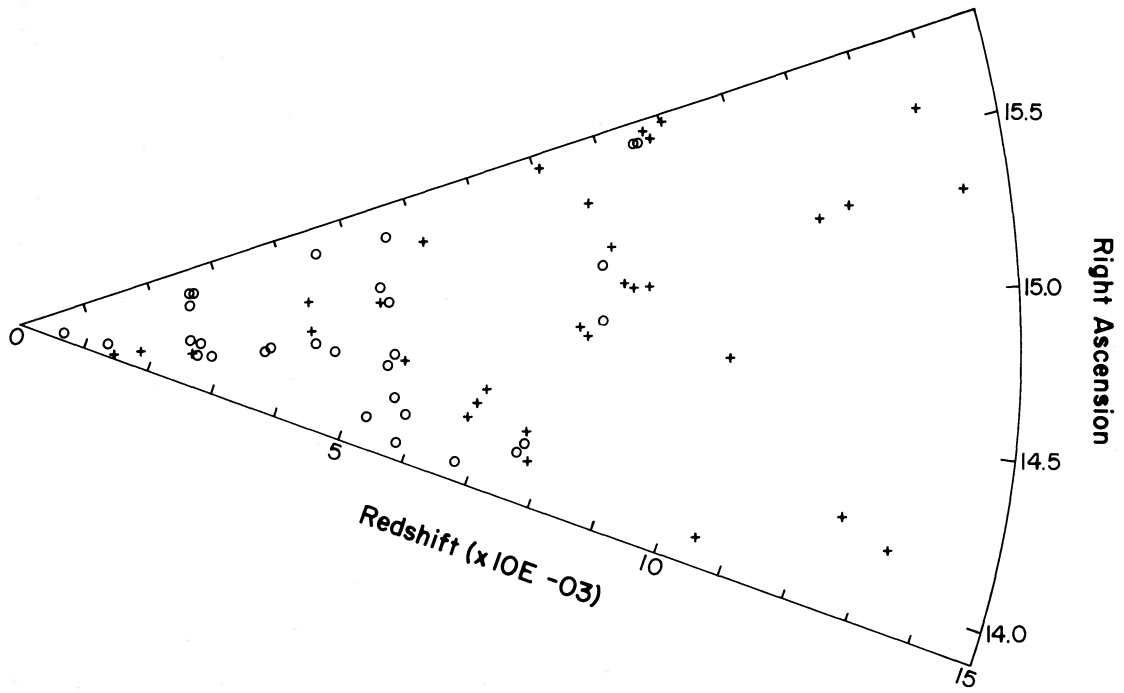

FIG. 4.—An expanded wedge diagram. The symbols are the same as in Fig. 3. The expanded redshift scale shows filamentary structures as discussed in the text.

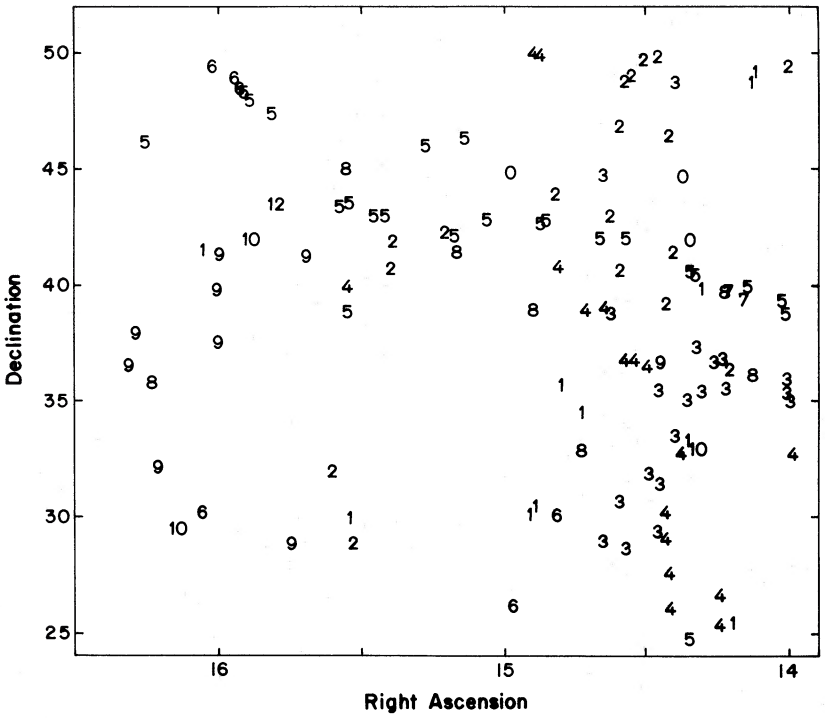

FIG. 5.—A map of the positions of CfA galaxies in an expanded region containing the SP sample. Galaxies are represented by one or two digits representing their redshifts (in km s^{-1}) trucated to 10^3 km s^{-1} units.

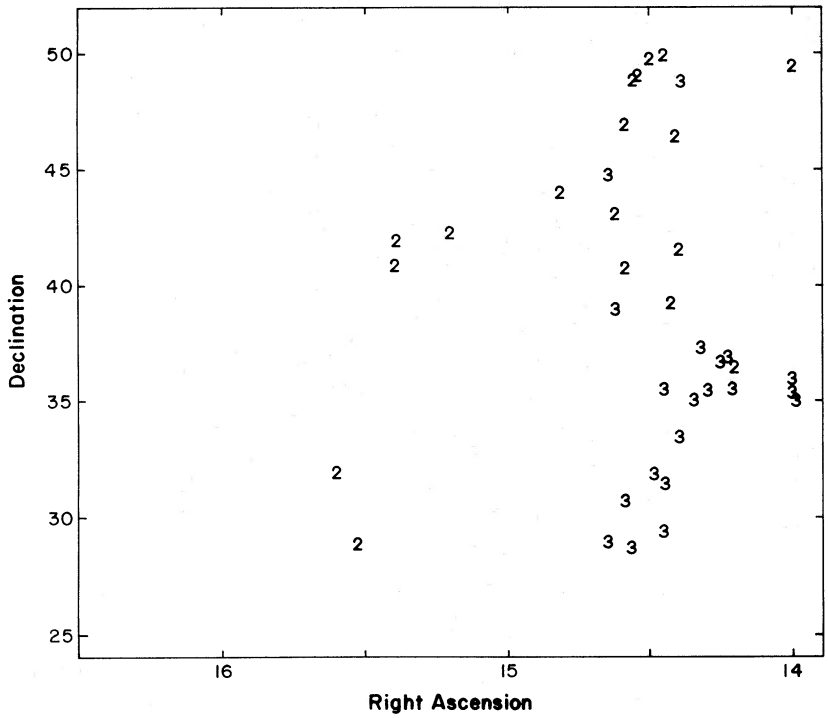

FIG. 6.—A redshift slice from Fig. 5. These CfA galaxies have redshifts of $2000 < V_0 < 3999$ km s^{-1}. Their distribution suggests a north-south running filament.

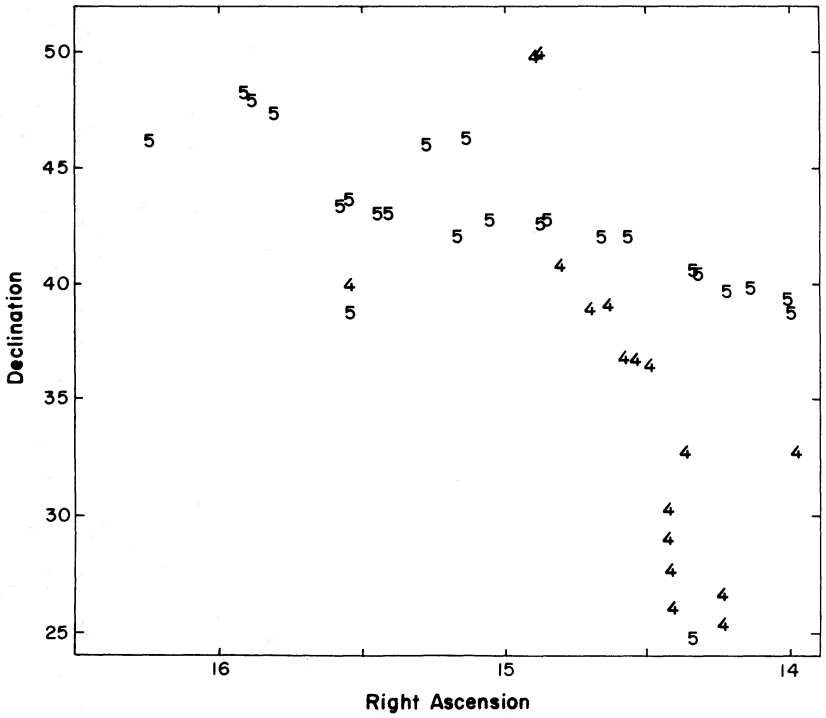

FIG. 7.—A second redshift slice from Fig. 5. These CfA galaxies have redshifts of $4000 < V_0 < 5999$ km s^{-1}. Their distribution suggest a 5 K filament running east-west and a 4 K filament running north-south. The 4 K filament mignt be associated with the 3 K filament seen in Fig. 6.

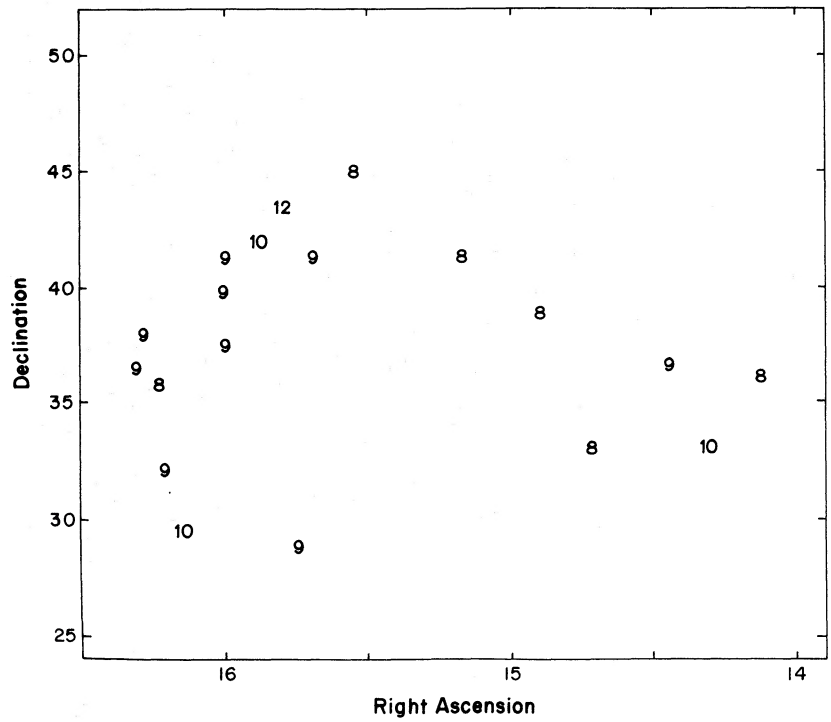

FIG. 8.—A third redshift slice from Fig. 5. These CfA galaxies have $8000 < V_0 < 12{,}999$ km s^{-1}. Their distribution suggests a 9–10 K filament running between $\alpha = 16^h3$, $\delta = 35°$ and $\alpha = 15^h5$, $\delta = 45°$. Galaxies to the west of this filament probably are not smoothly connected to it. The structures found in Figs. 5–8 help sort our structure in the SP data sample.

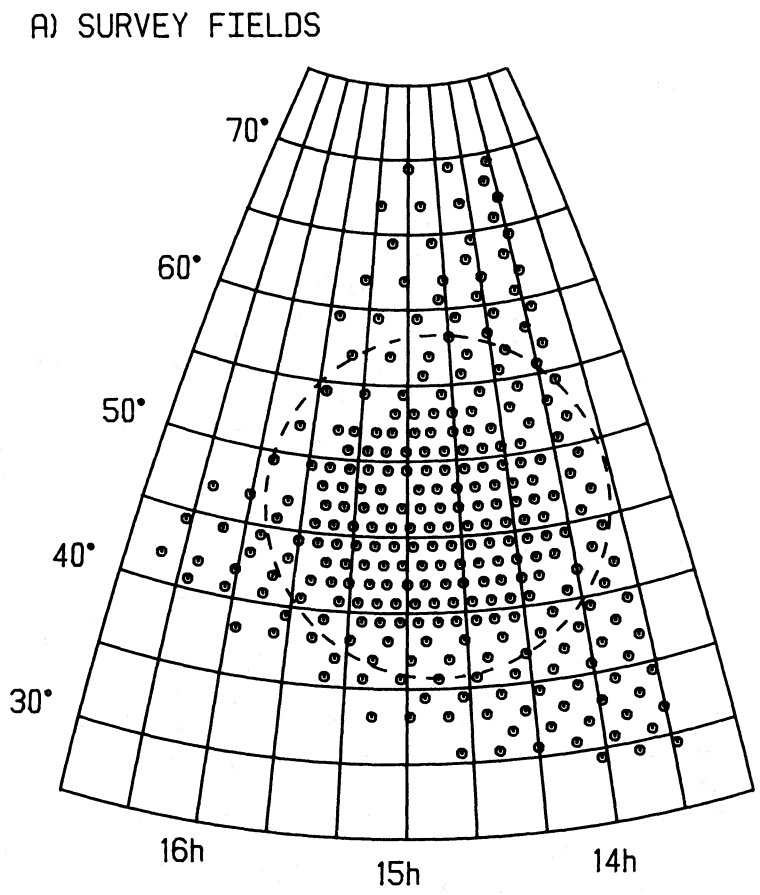

FIG. 9

FIG. 9.—(*a*) Positions on the sky of the 282 survey fields of KOSS83. (*b*) and (*c*) Positions of galaxies in two circle redshift ranges from 6000 to 18,000 km s^{-1} A circle denotes KOSS83 galaxies, and an X denotes SP galaxies. The dotted rectangle is the area searched by SP. The dashed circle is the projected 3000 km s^{-1} radius of the void at the distance of $cz = 15{,}000$ km s^{-1}.

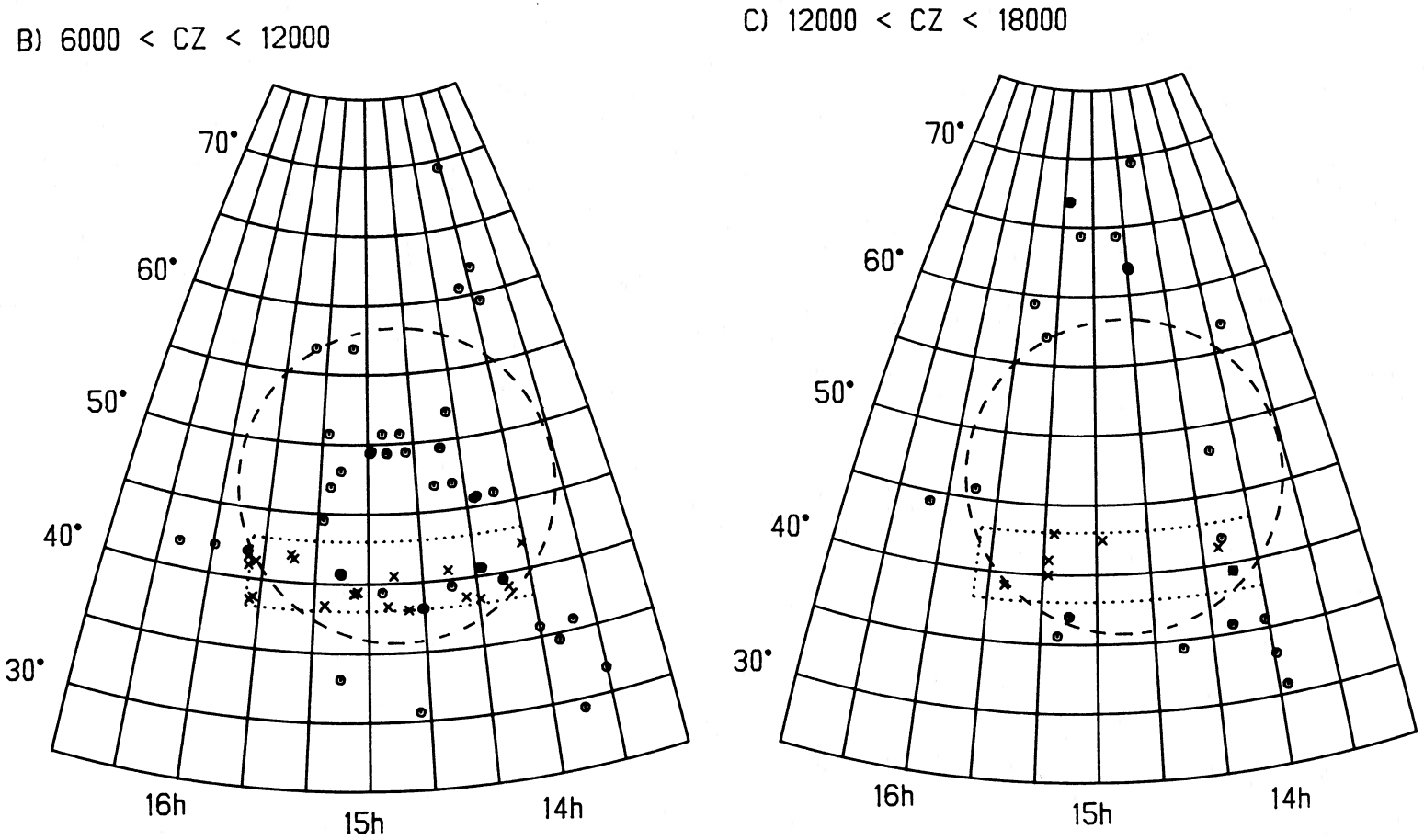

FIG. 9—*Continued*

e) Relation to the Bootes Void

A very important aspect of this survey is its relation to the giant void in Bootes. Again, because of the small number of SP galaxies, we will use other data to help define structure in and around the void region.

Kirshner *et al.* (1983, hereafter KOSS83; 1984, hereafter KOSS84) extended their original work by surveying 282 fields of area 0.0625 degree^2 (15′ × 15′ squares) laid out in a grid between the three fields of their original survey. The center of the grid was sampled at twice the density of the outer part as shown in Figure 9*a*. In Figures 9*b* and 9*c* we superpose the SP galaxies and field boundaries on their results. The two figures show where galaxies were discovered in the column in front of the void ($6000 < cz < 12{,}000$ km s^{-1}), and in the volume containing the void ($12{,}000 < cz < 18{,}000$ km s^{-1}). The dotted region represents the area searched by SP.

KOSS83 place the center of the void at $\alpha = 14^h48^m$, $\delta = +47°$ with a radius of approximately 3000 km s^{-1} which corresponds to an angular radius of 11°.3 (the dashed circle in Figs. 9*b* and 9*c*) at the void center distance of $cz = 15{,}000$ km s^{-1}. The SP survey area runs from 4° to 9° below the void center while stretching from edge to edge in right ascension. As shown in Figure 9*b*, closer than 12,000 km s^{-1} the SP galaxies appear to follow the distribution of the KOSS83 galaxies.

In Figure 9*c* the positional agreement of SP and KOSS83 galaxies is not as pronounced although one emissionless galaxy, SP 6 is common to both sets. Two galaxies, SP 29 and SP 40, having distances (converted from angular and redshift differences to symbolic velocity units) from the void center of 2742 and 2394 km s^{-1}, respectively, are found within the 3000 km s^{-1} radius described in KOSS83. Five others, SP 6, SP 7, SP 38, SP 41, and SP 50, have void distances between 3000 and 3300 km s^{-1} and thus lie at the void edge.

IV. DISCUSSION

There are two important aspects of this study. One is the question of what types of objects are found by the thin prism search technique. Of the 44 objects observed, 75% are confirmed emission-line extragalactic objects (two quasars and 31 galaxies). Of the remaining 11 (25%), six were found to have only absorption lines (three stars and three galaxies), and for five no emission was found in the Case search range (but might be present over a different spectral region). The overall success of this survey in identifying the desired objects is good and comparable with the 80% rate obtained with the Curtis Schmidt at CTIO by MacAlpine and collaborators (Lewis 1983).

The second aspect of this study is an alternative means of examining large-scale structure in the universe. Previous studies had usually been confined to magnitude limited samples which emphasize the most luminous galaxies. This type of sample generally showed filaments and voids (e.g., Tifft and Gregory 1976; Gregory and Thompson 1978; Gregory, Thompson, and Tifft 1981). The SP data provide a sample chosen in an independent manner with some very low luminosity galaxies included. There had been a previous suggestion that Markarian galaxies were distributed homogeneously (Balzano and Weedman 1982), although Thompson (1983) strongly suggested that the Markarian objects share the clumpy distribution of high-luminosity galaxies. Since the SP sample criterion was the presence of emission lines and the Markarian criterion was UV excess, the relationship of the two samples is not clear. However, Wasilewski (1983) has shown that a sample of emission-line galaxies chosen with somewhat higher dispersion plates than that of the SP sample has the same distribution as Markarian galaxies.

Our new data are consistent with the view that the SP galaxies are distributed in the same general manner as the CfA galaxies in Figures 5, 7, and 9 (although small number statistics make this statement difficult to quantify).

The nature of the Bootes void is not made much clearer by these results. Although two galaxies have been found within the void, several factors prohibit us from drawing conclusions about the density of the void or the fraction of emission lines galaxies in it. The first is that the SP survey center is placed 6°.5 below the void center. No galaxies could have been found closer than 1100 km s^{-1}, and if the void is spherical few would have been expected closer than 2000 km s^{-1}. Second, we do not know the depth of the SP survey and cannot calculate the expected number of galaxies if no void were present. This limitation is made worse by the inability of the SP technique to detect [O III] emission at $z > 0.06$. For large-scale structure purposes, it would be better to use a higher dispersion prism and redder sensitive emulsion (such as IIIa-F) so that galaxies with $M > M^*$ could be detected at distances greater than that of the void.

The SP sample has been shown to be useful in delineating large-scale structure although photometry of these galaxies is needed. The sample's lowest redshift galaxies add detail to nearby structures, and its higher redshift galaxies extend much farther out than the CfA catalog. The redshifts estimated by SP are reasonably accurate. It is likely that useful large-scale structure studies may be made from their whole catalogs. The sample also shows that this is an excellent technique for finding high-redshift quasars.

S. Gregory and R. Kirshner were supported in this research by NSF grants AST-8312791 and AST-8311414, respectively.

REFERENCES

Arakalyan, M. E., Dibai, E. A., and Esipov, V. F. 1972, *Astrofizika*, **8**, 33.
———. 1973*a*, *Astrofizika*, **9**, 319.
———. 1973*b*, *Astrofizika*, **9**, 325.
Balzano, V. A., and Weedman, D. W. 1982, *Ap. J. (Letters)*, **255**, L1.
Gregory, S. A., and Thompson, L. A. 1978, *Ap. J.*, **222**, 784.
Gregory, S. A., Thompson, L. A., and Tifft, W. G. 1981, *Ap. J.*, **243**, 411.
Huchra, J. Davis, M., Latham, D., and Tonry, J. 1983, *Ap. J. Suppl.*, **52**, 89 (CfA)
Huchtmeier, W. K., Richter, O.-G., Bohnenstengel, H.-D., and Haushildt, M. 1983, ESO Scientific Preprint 250.
Lewis, D. 1983, Ph.D. thesis, University of Michigan, Ann Arbor.
Kirschner, R. P., Oemler, A., Schechter, P. L., and Schectman, S. A. 1981, *Ap. J. (Letters)*, **248**, L57.
———. 1983, in *IAU Symposium 104, Early Evolution of the Universe and Its Present Structure*, ed. G. O. Abell and G. Chincarini (Dordrecht: Reidel), p. 197 (KOSS83).
———. 1984, in *Eleventh Texas Symposium on Relativistic Astrophysics*, ed. D. S. Evans, *Ann. Acad. Sci.*, **422**, 91 (KOSS84).
MacAlpine, G. M., and Lewis, D. W. 1978, *Ap. J., Suppl.*, **36**, 587.
MacAlpine, G. M., Lewis, D. W., and Smith, S. B. 1977, *Ap. J. Suppl.*, **35**, 203.
MacAlpine, G. M., Smith, S. B., and Lewis, D. W. 1977*a*, *Ap. J. Suppl.*, **34**. 95.
———. 1977*b*, *Ap. J. Suppl.*, **35**, 197.

Minkowski, R. 1961, *A. J.*, **66**, 558.
Moody, J. W. 1986, Ph.D. thesis, the University of Michigan, Ann. Arbor.
Sanduleak, N., and Pesch, P. 1982, *Ap. J. (Letters)*, **258**, L11 (SP).
———. 1983, *Ap. J. Suppl.*, **51**, 171.
———. 1984, *Ap. J. Suppl.*, **55**, 517.
Sargent, W. L. W., and Searle, L. 1970, *Ap. J. (Letters)*, **162**, L155.
Smith, M. G. 1975, *Ap. J.*, **202**, 591.
Thompson, L. A. 1983, *Ap. J.*, **266**, 446.
Tifft, W. G., and Gregory, S. A. 1976, *Ap. J.*, **205**, 696.
Wasilewksi, A. J. 1983, *Ap. J.*, **272**, 68.

STEPHEN A. GREGORY: Department of Physics and Astronomy, University of New Mexico, Albuquerque, NM 87131

ROBERT P. KIRSHNER: Department of Astronomy, Harvard University, Cambridge, MA 02138

J. WARD MOODY: Department of Astronomy, University of Michigan, Ann Arbor, MI 48109

WILLIAM G. TIFFT: Steward Observatory, University of Arizona, Tucson, AZ 85721